Development of an Airborne Integrated Phase Doppler Interferometer/Imaging Probe for Accurate Cloud Droplet Size Distribution Measurement

Topic # N02-061

Contract No.
N00014-02-M-0153

Final Technical Report

For period covering
June 1, 2002 – September 30, 2002

Submitted to
Office of Naval Research
800 North Quincy Street
Arlington, VA 22217-5660

Principal Investigator
William D. Bachalo

Artium Technologies, Inc.
150 West Iowa Avenue, Suite 202
Sunnyvale, CA 94086

November 12, 2002

Unlimited/Unclassified

1. Phase I Objective

The objective of the Phase I program was to investigate the feasibility of developing an optical probe based on phase Doppler interferometry (PDI) for reliable and accurate measurement of the cloud droplet size distribution from airborne platforms. The key features of this device are high accuracy and precision droplet sizing, large dynamic range, accurate concentration measurement throughout the entire instrument dynamic range, very low coincidence errors, and large counting volume. The other key features of the instrument are: low cost, low power consumption, compactness, and real-time data monitoring and transmission to ground-based facilities. Additional tasks include the investigation of methods the discrimination of ice crystals from water drops, and subsequent imaging of these particles. The integration of the imaging probe with a phase-Doppler system will permit measurement of both spherical and non-spherical particles. Toward this end, the Phase I program, including the Phase I Option, had the following specific goals:

- Identify, select, and evaluate advanced electro-optical components that would permit a compact, low-cost PDI probe design for cloud droplet distribution measurements.

- Quantify and/or verify key PDI performance characteristics such as sizing accuracy, concentration accuracy, dynamic range, and probe volume that are important for reliable measurements in clouds.

- Develop algorithms to minimize coincidence by separating partially (but not totally) overlapping droplets.

- Investigate the feasibility of using a polarization technique for discriminating between solid ice crystals and liquid droplets.

- Investigate the feasibility of using a novel multi-laser beam technique for shadowing individual droplets and ice-crystals on to a 2-D CCD array.

- Identify suitable signal processing approaches for reliably and accurately measuring the particle size and morphology using the imaging probe.

2

- Investigate the feasibility of integrating the imaging probe to a PDI to yield a hybrid instrument that would be suitable for aircraft-based cloud particle characterization and provide a large (200:1) sizing dynamic range.

- Investigate suitable software methodologies for real-time processing of the PDI and Imaging probe data, correcting for particle size dependent probe volume sizes, extracting the liquid water content, computing the particle size distribution, correlating this data to the onset of icing on aircraft, and transmitting this information from airborne platforms to earth-based monitoring stations.

2. Description of Work Performed in Phase I

Task 1: Selection of suitable solid-state lasers

To-date, conventional phase-Doppler systems, cloud characterization systems, and other particle imaging systems have used gas phase lasers such as He-Ne or Ar-ion (water-cooled or air-cooled). These lasers are bulky, consume a lot of power, and are inefficient. More recently, tremendous advances have been made in the area of diode lasers. With their widespread use in fiber-optics telecommunication systems, a large number of compact, reliable, and low-cost diode laser are now available commercially. Furthermore, advances have also been made in the area of diode-pumped solid-state (e.g. Nd:YAG) lasers. The diode-pumped lasers are compact, relatively low-cost, provide high power, possess excellent coherence lengths, are available in different wavelengths, and in general, are ideally suited for phase-Doppler systems. The use of diode lasers or diode-pumped solid-state lasers will allow us to achieve a compact design for the aircraft-based cloud probe without the need for single-mode polarization preserving fiber optics. Furthermore, the power consumption of these lasers is also much less than for conventional gas lasers.

During the Phase I program, we reviewed the commercial availability of different solid state lasers and selected a suitable laser for aircraft-based PDI and imaging probes. Some of the key features that were examined include beam quality, coherence, stability, laser power, electrical

3

power requirements, beam divergence and wavelength. Table I summarizes the various commercially available diode lasers and their specifications:

Company	Laser Model	Power	Wavelength	Price	Linewidth	Freq. Drift	Polarization	RMS Noise	M^2	Beam Dia.	Divergence	Power Stability	Pointing Stability	Ellipticity/Round	Head Dim. mm
JDS Uniphase	CPDS532S-010	10 mW	532 ± 1 nm	-	-		>100:1	< 0.5%	< 1.3	1.9 ± 0.2 mm	<1.2 mrad	< 1.5%	± 30 µrad	<10%	28.86x39.83x76.2
	CPDS532S-020	20 mW	532 ± 1 nm	-	-		>100:1	< 0.5%	< 1.3	1.9 ± 0.2 mm	<1.2 mrad	< 1.5%	± 30 µrad	<10%	28.86x39.83x76.2
	CDPS532M-010	10 mW	532 ± 1 nm	-	-		>100:1	< 0.5%	< 1.2	0.6 mm ±10%	<1.2 mrad	< 1.0%	± 30 µrad	<10%	38.1x38.1x101.6
	CDPS532M-020	20 mW	532 ± 1 nm	-	-		>100:1	< 0.5%	< 1.2	0.6 mm ±10%	<1.2 mrad	< 1.0%	± 30 µrad	<10%	38.1x38.1x101.6
	CDPS532M-050	50 mW	532 ± 1 nm	-	-		>100:1	< 0.5%	< 1.2	0.6 mm ±10%	<1.2 mrad	< 1.0%	± 30 µrad	<10%	38.1x38.1x101.6
Coherent	Verdi-V10	10 W	532 nm	-	< 5Mhz		>100:1	< 0.1%	< 1.1	2.25 mm +-10%	<0.5 mrad	+/- 1%	< 5 µrad/°C	-	108.7x139.7x464.3
	Verdi-V8	8 W	532 nm	-	< 5Mhz		>100:1	< 0.1%	< 1.1	2.25 mm +-10%	<0.5 mrad	+/- 1%	< 5 µrad/°C	-	108.7x139.7x464.3
	Verdi-V6	6 W	532 nm	-	< 5Mhz		>100:1	< 0.02%	< 1.1	2.25 mm +-10%	<0.5 mrad	+/- 1%	< 5 µrad/°C	-	108.7x139.7x464.3
	Verdi-V2	2 W	532 nm	-	< 5Mhz		>100:1	< 0.02%	< 1.1	2.25 mm +-10%	mrad +/- 1	+/- 1%	< 5 µrad/°C	>95%	108.7x139.7x464.3
	Compass 215M-10	10 mW	532 nm	-	-		100:1	<0.5%	<1.1	0.32 mm ±10%	<2.5 mrad	<±2%	<6 µrad/°C	1.05:1 / >95%,	33 x 42 x 100
	Compass 215M-15	15 mW	532 nm	-	-		100:1	<0.5%	<1.1	0.32 mm ±10%	<2.5 mrad	<±2%	<6 µrad/°C	1.05:1 / >95%,	33 x 42 x 100
	Compass 215M-20	20 mW	532 nm	-	-		100:1	<0.5%	<1.1	0.32 mm ±10%	<2.5 mrad	<±2%	<6 µrad/°C	1.05:1 / >95%,	33 x 42 x 100
	Compass 215M-50	50 mW	532 nm	-	-		100:1	<0.5%	<1.1	0.32 mm ±10%	<2.5 mrad	<±2%	<6 µrad/°C	1.05:1 / >95%,	33 x 42 x 100
	Compass 215M-75	75 mW	532 nm	-	-		100:1	<0.5%	<1.1	0.32 mm ±10%	<2.5 mrad	<±2%	<6 µrad/°C	1.05:1 / >95%,	33 x 42 x 100
	Compass 315M-20	20 mW	532 nm	-	-		100:1	<0.25%	-	0.32 ±0.02 mm	<2.2 mrad	<±2%	<6 µrad/°C	<1.1:1.0 / >95%,	32.5 x 40 x 100
	Compass 315M-50	50 mW	532 nm	-	-		100:1	<0.25%	-	0.32 ±0.02 mm	<2.2 mrad	<±2%	<6 µrad/°C	<1.1:1.0 / >95%,	32.5 x 40 x 100
	Compass 315M-100	100 mW	532 nm	-	-		100:1	<0.25%	-	0.32 ±0.02 mm	<2.2 mrad	<±2%	<6 µrad/°C	<1.1:1.0 / >90%,	32.5 x 40 x 100
	Compass 315M-150	150 mW	532 nm	-	-		100:1	<0.25%	-	0.34 ±0.02 mm	<2.2 mrad	<±2%	<6 µrad/°C	<1.1:1.0 / >90%,	32.5 x 40 x 100
	Compass 415M-200	200 mW	532 nm	-	-		100:1	<0.25%	-	0.345 ±0.015 mm	<3 mrad	<±2%	<6 µrad/°C	<1.1:1.0 / >90%,	33 x 66 x 190
	Compass 415M-300	300 mW	532 nm	-	-		100:1	<0.25%	<1.1	0.355 ±0.015 mm	<3 mrad	<2%	<6 µrad/°C	<1.1:1.0 / >90%	33 x 66 x 190
	Sapphire 460-10	10 mW	460 ±2 nm	-	-		>100:1	<0.25%	<1.1	0.70 ±0.05 mm	<1.2 mrad	<2%	<30 µrad	<1:1.1	34 x 70 x 125
	Sapphire 488-20	20 mW	488 ±2 nm	-	-		>100:1	<0.25%	<1.1	0.70 ±0.05 mm	<1.2 mrad	<2%	<30 µrad	<1:1.1	34 x 70 x 125
Crystalaser	GCL-005-S	5 mW	532 nm	$4,500	< 20 kHz (< 10^-5 nm)	100 Mhz over one hour	> 100 :1	< 0.5%	-	0.36 mm	2 mrad	2% or <0.25%	< 0.02 mrad	-	30 x 30 x 120
	GCL-025-S	25 mW	532 nm	$5,732	< 20 kHz (< 10^-5 nm)	100 Mhz over one hour	> 100 :1	< 0.5%	-	0.36 mm	2 mrad	2% or <0.25%	< 0.02 mrad	-	30 x 30 x 120
	GCL-050-S	50 mW	532 nm	$7,492	< 20 kHz (< 10^-5 nm)	100 Mhz over one hour	> 100 :1	< 0.5%	-	0.36 mm	2 mrad	2% or <0.25%	< 0.02 mrad	-	30 x 30 x 120
	GCL-075-S	75 mW	532 nm	$9,287	< 20 kHz (< 10^-5 nm)	100 Mhz over one hour	> 100 :1	< 0.5%	-	0.36 mm	2 mrad	2% or <0.25%	< 0.02 mrad	-	30 x 30 x 120
	GCL-100-S	100 mW	532 nm	$11,475	< 20 kHz (< 10^-5 nm)	100 Mhz over one hour	> 100 :1	< 0.5%	-	0.36 mm	2 mrad	2% or <0.25%	< 0.02 mrad	-	30 x 30 x 120
	GCL-150-S	150 mW	532 nm	$15,227	< 20 kHz (< 10^-5 nm)	100 Mhz over one hour	> 100 :1	< 0.5%	-	0.36 mm	2 mrad	2% or <0.25%	< 0.02 mrad	-	30 x 30 x 120
	GCL-200-S	200 mW	532 nm	$18,900	< 20 kHz (< 10^-5 nm)	100 Mhz over one hour	> 100 :1	< 0.5%	-	0.36 mm	2 mrad	2% or <0.25%	< 0.02 mrad	-	30 x 30 x 120
	BCL-002-L	2 mW	473nm	$5,400	0.1 nm	-	> 50 :1	5% or 1%	-	0.2 mm	3.6 mrad	2% or <0.25%	0.02 mrad	-	30 x 30 x 120
	BCL-005-L	5 mW	473nm	$6,950	0.1 nm	-	> 50 :1	5% or 1%	-	0.2 mm	3.6 mrad	2% or <0.25%	0.02 mrad	-	30 x 30 x 120
	BCL-010-L	10 mW	473nm	$9,990	0.1 nm	-	> 50 :1	5% or 1%	-	0.2 mm	3.6 mrad	2% or <0.25%	0.02 mrad	-	30 x 30 x 120
	BCL-015-L	15 mW	473nm	$12,990	0.1 nm	-	> 50 :1	5% or 1%	-	0.2 mm	3.6 mrad	2% or <0.25%	0.02 mrad	-	30 x 30 x 120

Company	Laser Model	Power	Wavelength	Price	Linewidth	Freq. Drift	Polarization	RMS Noise	M^2	Beam Dia.	Divergence	Power Stability	Pointing Stability	Elliptical y/Round	Head Dim. mm
sverse s Co., Ltd.	TIM-622C	?	532 nm	-	<0.05 nm	-	> 100:1	-	-	< 3.5 mm	<3 mrad	5% - 10%	-	-	60 x 66 x 110
	TIM-622-[10-150]	0 - 150 mW	532 nm	-	<0.05 nm	-	> 100:1	-	-	< 2.5 mm	<2 mrad	-	< 0.02 mrad	-	92 x 102 x 143
twave ronics	142S-532-100	100 mW	532 nm	-	<10 kHz/msec	-	>100:1	<0.2%	<1.1	0.42 mm nominal	mrad nom	<5%	<0.1 mrad	<10% elliptical	60 x 80 x 200
	142S-532-200	200 mW	532 nm	-	<10 kHz/msec	-	>100:1	<0.2%	<1.1	0.42 mm nominal	mrad nom	<5%	<0.1 mrad	<10% elliptical	60 x 80 x 200
	142S-532-300	300 mW	532 nm	-	<10 kHz/msec	-	>100:1	<0.2%	<1.1	0.42 mm nominal	mrad nom	<5%	<0.1 mrad	<10% elliptical	60 x 80 x 200
Vision ologies,	JLM-3	3mW	532 nm	-	-	-	-	-	-	-	<1.2 mrad	<±20% at 25°C-30°C	-	-	21 x 21 x 50
	JLM-5	5mW	532 nm	-	-	-	-	-	-	-	<1.2 mrad	<±20% at 25°C-30°C	-	-	21 x 21 x 50
	JLM-10	10mW	532 nm	-	-	-	-	-	-	-	<1.2 mrad	<±20% at 25°C-30°C	-	-	21 x 21 x 50
	JLM-20	20mW	532 nm	-	-	-	-	-	-	-	<1.2 mrad	<±20% at 25°C-30°C	-	-	21 x 21 x 50
wer logy, Inc.	LCS-DTL-312-50	50 mW	532	-	-	-	>100:1	-	-	1.5	0.4 mrad	2%	-	-	46x90x225
	LCS-DTL-312-100	100 mW	532	-	-	-	>100:1	-	-	1.5	0.4 mrad	2%	-	-	46x90x225
	LCS-DTL-312-150	150 mW	532	-	-	-	>100:1	-	-	1.5	0.4 mrad	2%	-	-	46x90x225
	LCS-DTL-312-200	200 mW	532	-	-	-	>100:1	-	-	1.5	0.4 mrad	2%	-	-	46x90x225
s Griot	58 GCS 405	5 mW	2 nm +/- 1.0	$3,442	-	-	-	<2%	-	1.180.2 mm	1.25 mrad	+/- 4%	0.02 mrad/°	<1.1:1	64 x 80.8 x 130.3
	58 GCS 411	10 mW	2 nm +/- 1.0	$5,592	-	-	-	<2%	-	1.180.2 mm	1.25 mrad	+/- 4%	0.02 mrad/°	<1.1:1	64 x 80.8 x 130.3
	58 GCS 421	20 mW	2 nm +/- 1.0	$6,391	-	-	-	<2%	-	1.180.2 mm	1.25 mrad	+/- 4%	0.02 mrad/°	<1.1:1	64 x 80.8 x 130.3
rshop	EJLM-3	3 mW	532 nm	$285	-	-	-	-	-	-	1.2 mrad	+/- 20%	-	-	21x21x50
	EJLM-5	5 mW	532 nm	$295	-	-	-	-	-	-	1.2 mrad	+/- 20%	-	-	21x21x50
	EJLM-10	10 mW	532 nm	$345	-	-	-	-	-	-	1.2 mrad	+/- 20%	-	-	21x21x50
	EJLM-20	20 mW	532 nm	$675	-	-	-	-	-	-	1.2 mrad	+/- 20%	-	-	21x21x50
te, Inc.	GSLN32-20	mW adjust	532 nm	$5,995	-	-	> 100:1	< 1 %	-	0.4 mm	1.5 mrad	< 1%	< 0.05 mrad	-	46 x 90 x 225
	GSLN32-50	mW adjust	532 nm	$7,995	-	-	> 100:1	< 1 %	-	0.4 mm	1.5 mrad	< 1%	< 0.05 mrad	-	46 x 90 x 225
	GSF32-5P	5 mW	532 nm	$1,695	-	-	-	-	-	1.0 mm	0.6 mrad	< 2%	< 0.05 mrad	-	45 x 60 x 120
	GSF32-10P	10 mW	532 nm	$1,895	-	-	-	-	-	1.0 mm	0.6 mrad	< 2%	< 0.05 mrad	-	45 x 60 x 120
	GSF32-20P	20 mW	532 nm	$2,495	-	-	-	-	-	1.0 mm	0.6 mrad	< 2%	< 0.05 mrad	-	45 x 60 x 120
	GSF32-50P	50 mW	532 nm	$4,995	-	-	> 100:1	-	-	1.5 mm	0.4 mrad	< 2%	< 0.05 mrad	-	46 x 90 x 225
	GSF32-100P	100 mW	532 nm	$5,595	-	-	> 100:1	-	-	1.5 mm	0.4 mrad	< 2%	< 0.05 mrad	-	46 x 90 x 225
	GSF32-150P	150 mW	532 nm	$5,995	-	-	> 100:1	-	-	1.5 mm	0.4 mrad	< 2%	< 0.05 mrad	-	46 x 90 x 225
	GSF32-200P	200 mW	532 nm	$6,995	-	-	> 100:1	-	-	1.5 mm	0.4 mrad	< 2%	< 0.05 mrad	-	46 x 90 x 225
	BSF73-10I	10 mW	473 nm	$5,495	-	-	> 100:1	-	-	1.5 mm	0.5 mrad	< 2%	< 0.05 mrad	-	46 x 90 x 225
	BSF73-20I	20 mW	473 nm	$6,495	-	-	> 100:1	-	-	1.5 mm	0.5 mrad	< 2%	< 0.05 mrad	-	46 x 90 x 225
	BSF73-30I	30 mW	473 nm	$7,495	-	-	> 100:1	-	-	1.5 mm	0.5 mrad	< 2%	< 0.05 mrad	-	46 x 90 x 225
	BSF73-40I	40 mW	473 nm	$8,495	-	-	> 100:1	-	-	1.5 mm	0.5 mrad	< 2%	< 0.05 mrad	-	46 x 90 x 225

Task 2: Investigate the use of large area avalanche photodiodes to extend dynamic range Solid state detectors

Conventional phase Doppler systems, including icing/cloud probes, incorporate photomultiplier tubes as optical detectors. The main advantage of the PMT is its high frequency response. Unfortunately, the dynamic range offered by the PMTs are restricted to approximately 2500:1. Furthermore, it is well known that light scattered by spherical particles that are larger than the wavelength of light varies as the square of its diameter. Therefore, for a particular PMT high voltage setting, the detectable particle size range is approximately 50:1. This means that if the PDI system is configured to measure a particle that is 3 µm in diameter then the largest droplet that it can measure is 150 µm. Particles larger than 150 microns will saturate the PMT and will not be processed. This limits the size range over which cloud droplet size distribution measurements can be made, unless an increase in the system dynamic range can be implemented.

In phase I, several schemes to improve the size dynamic range of PDI systems were evaluated. Two approaches were examined to achieve this task: electrical and optoelectronics. Electrical means, including preamplification configurations and phototdetectors such as the large area avalanche photodiodes (LAAPD), were examined in the first approach. The performance of these schemes was tested for optimum performance. In the second approach, the feasibility of using different optoelectronic modulators was evaluated.

Figure 1 shows the block diagram of the setup used to evaluate the different configurations for the first approach. It comprises of a photodetector to convert the optical signal into current, a transimpedance amplifier to convert the current into voltage and a voltage control gain or automatic gain amplifier (AGC).

Traditionally, the transimpedance amplifier output is fed directly to the PDI processor. This limits the minimum detectable PDI signal level by the noise level on the common ground of the detector/preamplifier and the processor. This ground noise can reach several millivolts due to the large bandwidth (in excess of 100 MHz) required for PDI system. This, in turn, limits the dynamic range to 1:1000 to 1:2500 even in well-designed systems. The use of automatic gain

controllers (AGC's) to amplify the signal before feeding it to processor was examined in this program to overcome the limited dynamic range problem.

To test the different schemes, a circuitry that generates simulated optical Doppler signals was developed. This was achieved by modulating a laser diode by simulated Doppler signals. A variable optical attenuator was then used to attenuate the laser diode optical signal over the range (0-40 dB) (0dB represent no attention, 33 dB represent attenuation by a factor 2500, 40dB represent attenuation a factor 10000).
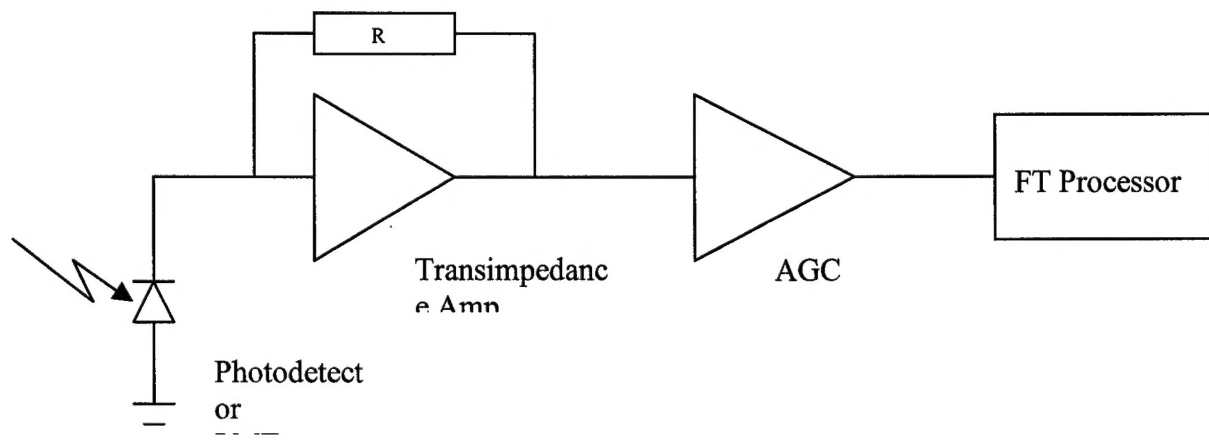
Figure 1: Block diagram of the circuit used for evaluation.

The laser diode signal after attenuation was used as input for each approach under test. The Signal-to-Noise Ratio (SNR) of the electrical signal at the output was measured. This was achieved by sampling the signal and then computing the power spectrum of the sampled data using 1024 samples. The SNR was measured by dividing the peak power (signal power) by the sum of the power spectrum excluding the peak (noise power). The dynamic range was determined by the optical attenuation that gave SNR equal to the minimum detectable SNR of the signal processor. For the developed processor (ASA) under this program, this value is –6 dB. However, it should be pointed out that conventional PDI processors have a minimum SNR higher than –6 dB and therefore the dynamic range for these systems will be less that what we are reporting here.

Several voltage-controlled gain or AGC amplifier were tested and their performance for PDI applications were evaluated. To be suitable for PDI applications, the phase of the amplifier output should not vary with varying the gain through the control voltage. To test for this condition, a simulated Doppler signal with frequencies over the range 20 to 100 MHz was applied to each amplifier. The phase of the signal output was measured with respect to the input signal. The gain of the amplifier was then varied by varying the control voltage over its specified dynamic range. The phase of the amplifier output signal should not vary by more than one degree over the its specified dynamic range. With these test criteria, it was determined that AD8367 provides satisfactory performance for our application.

The specifications of the Large Area APD's (LAAPD) from different vendors were reviewed. For PDI applications, the primary concern is the frequency response and the effective area of these detectors. It was determined, that LAAPD's with active areas large than 2mm do not provide sufficient bandwidth for PDI applications. The bandwidth for such detectors is less than 100 MHz. On the other hand, the use of LAAPD's with active areas less than 0.5 mm will complicate the receiver design. This results from the difficulties in directing the light into the APD active area. LAAPD's with active areas of 1 mm provides the best compromise. Its bandwidth is greater than 200 MHz and it can be integrated into the receiver without great difficulty. The APD evaluation board model number C5331 from Hamamatsu was selected and used for evaluating LAAD performance. The APD in this module has an effective area of 1 mm.

Figure 2 shows the experimental results for four different configurations to determine the one with the highest dynamic range. The first configuration represents the conventional scheme where a PMT (RU5600 from Hamamatsu) followed by a transimpedance amplifier was used. The dynamic range for this configuration could barely meet the required dynamic range of 1:2500. Notice that for a processor with a minimum SNR of 0 dB, the dynamic range will be reduced to less than 1:1000. In the second configuration, AGC AD8367 was added at the output of the first configuration. The test results show that the dynamic range was improved by 50% to 1:3500. For configurations 3 and 4, an LAAPD from Hamamatsu was used. In the third configuration, a transimpedance amplifier was used without AGC. The dynamic range was 1:3000 slightly less than that of configuration 2. Although the use of LAAPD instead of PMT

improved the system performance, the real improvement came from using *both LAAPD and AGC* as shown in configuration 4. The dynamic range for configuration was 1:8000. This result is close to our goal of 1:10000.
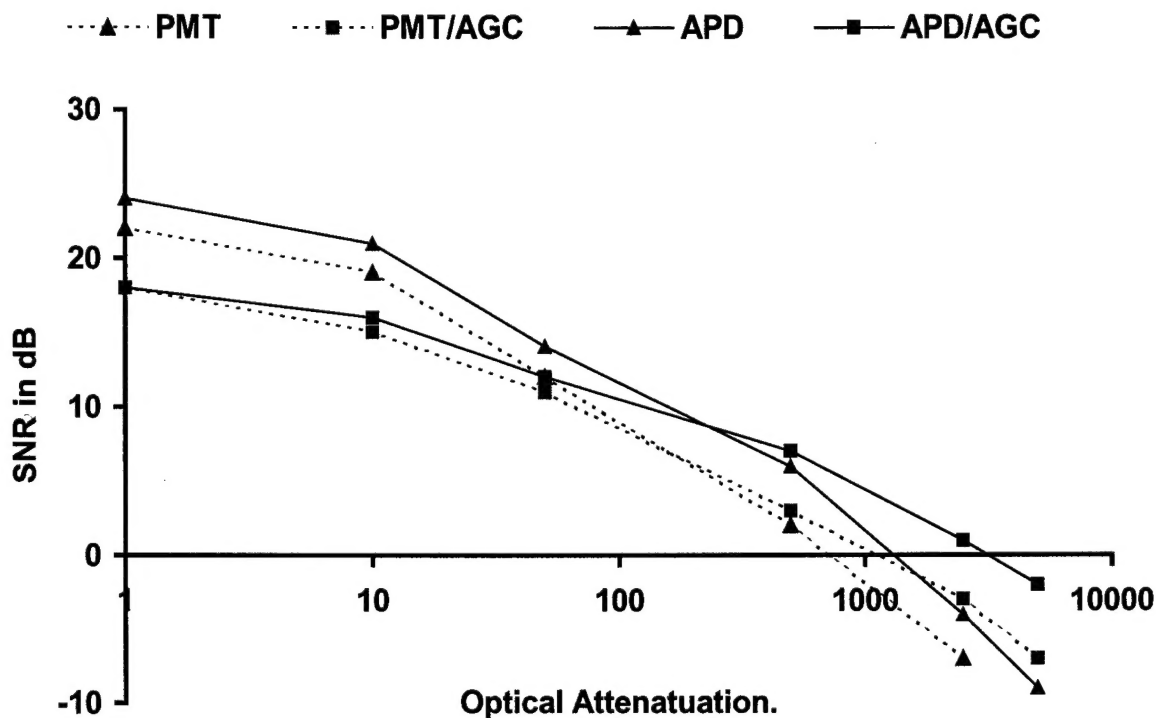
Figure 2: SNR in dB of the four different confiurations vs optical attenaution.

Task 3: Develop electro-optical means to further extend the dynamic range

Besides the use of the LAAPD and AGC we also investigate the feasibility of using electro-optical means for further extending the size dynamic range of the PDI cloud probe. Some possibilities include the use of acousto-optic deflectors (Bragg cells) or high-speed electro-optic modulators, such as Kerr cells or Pockels cells, to dynamically attenuate the intensity of the incident laser beam or the scattered light to prevent the PMT from saturating when large droplets pass through the PDI measurement probe volume. Such a dynamic attenuation scheme can either be implemented in the transmitter side or on the receiver side of the PDI probe.

We encountered a setback in our search for a suitable electro-optical modulation technique for increasing the PDI size dynamic range. The use of Mach-Zender modulators and electro-absorption modulators were eliminated because of the very narrow bandwidth over which they can operate and due to the non-availability of such devices in the visible spectrum. Even if these problems were overcome, it would be difficult to integrate them into the receiver. The use of Pockel cells was also eliminated. These cells can't operate when the modulating signal (Doppler signal pedestal) transit times varies over a factor of 10 or more.

Instead of electro-optical modulators, we are now investigating the feasibility of using a acousto-optical modulator (a Bragg cell) for increasing the size dynamic range. With this approach, the RF signal used to drive the Bragg cell will be modulated by the Doppler signal pedestal. Thus, the power of the primary laser will be changed (or modulated) by the amplitude of the Doppler signal pedestal. This approach will be further investigated in the Phase II program.

In any case, we feel confident that a combination of the three approaches (pre-amplifier gain, LAAPD and/or acousto-optic modulation) will allow for an increase in the PDI size dynamic range from 50:1 to at least 100:1. As stated in the previous section, the combination of an AGC and LAAPD already gives us a dynamic range of approximately 90:1.

Task 4: Methods for accurate measurement of cloud droplet size distribution

In the Phase I program various techniques were identified to provide improved accuracy in the measurement of the cloud droplet size distribution. These techniques are described in this section.

Theoretical Simulations

In the past, we have developed extensive theoretical models, based both on the geometrical optics theory and the more comprehensive Lorenz-Mie light scattering theory, to compute the PDI phase-vs-size response curves. Several technical paper have been presented and published by the PI, Dr. Bachalo, and Dr. Sankar on this subject. During the current reporting period, we enhanced the geometrical optics models to simulate the time varying Doppler signals for a droplet passing through a specified trajectory in the measurement probe volume. A typical Doppler signal simulation is shown in Fig.3. In Fig.3, each of the three Doppler signals represent

the analog output of the three spatially separated photodetector located in the optical receiver of a PDI system. In PDI, the phase difference between any two detectors is measured and used to infer the droplet size.

Conventional PDI systems provide only a single measure of the phase difference for each droplet. However, we have determined that due to the complexity of the light scattering process (scattered light consists of reflected and multiple orders of refracted rays), the phase difference actually varies as a function of time. We are currently trying to use the theoretical models to clearly demonstrate this phenomenon. Having clearly established this fact, we will be investigating signal-processing techniques that can extract the phase-difference at different instants in time. Further, this information will be used to establish confidence in the size measurement. Specifically, we will be developing validation criteria that will help reject those signals that pass through certain undesirable edge trajectories causing erroneous measurements. To take it one step further, we will also be investigating means of extracting the correct size from the edge-trajectory Doppler signals. Overall, this will lead to improved accuracy in the measured size distribution and also in the measured liquid volume flux. We believe this is a patentable idea and will file for one once we have satisfactorily investigated the idea. This idea will be further pursued and enhanced in the Phase II program.
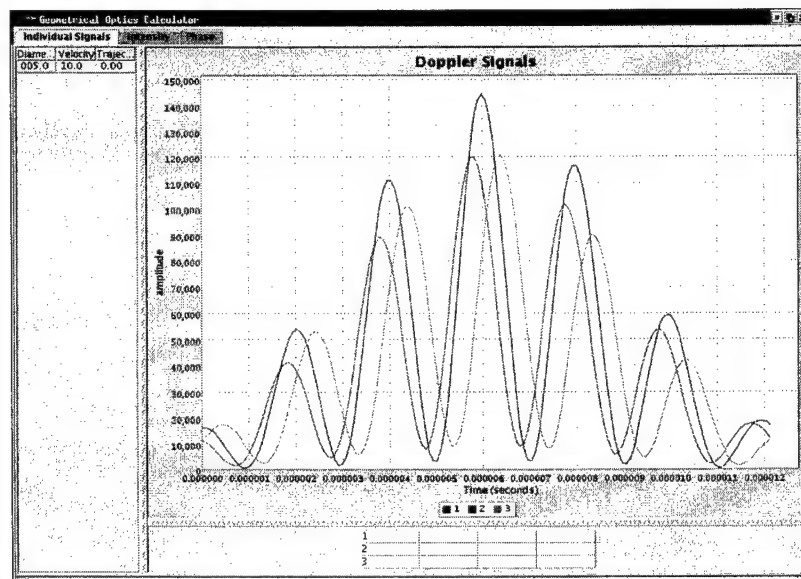
**Figure 3:** Simulated Doppler signals.

Tophat Beam

The laser intensity profile within the measurement probe volume is typically Gaussian in nature. In the past, we have demonstrated that the use of a Gaussian profile will give rise to trajectory-dependent errors. Basically, large particles passing through certain edge-trajectories are erroneously measured. In the previous section we discussed our modeling efforts that was aimed at identifying and correcting such errors. Another method to minimize trajectory dependent errors is to create a "top hat" beam profile in the measurement probe volume. We have successfully done this with another product of ours, namely the LII (laser induced incandescence) system.

In the LII, we employed two techniques to optimize the uniformity of the laser beam at the probe volume:

- We expand the beam into a sheet and used an iris to restrict the field-of-view to the central portion of the beam (the iris allows us to vary the probe volume size, and thus signal intensity);

- We used a vertical-slit aperture to pass just the central portion of the beam in the depth-of-field direction, and relay image the slit plane to the probe volume.

Figure 4 shows a typical "top hat" beam profile obtained in our LII system. We will employ a similar approach to create a "top hat" beam in our PDI system.
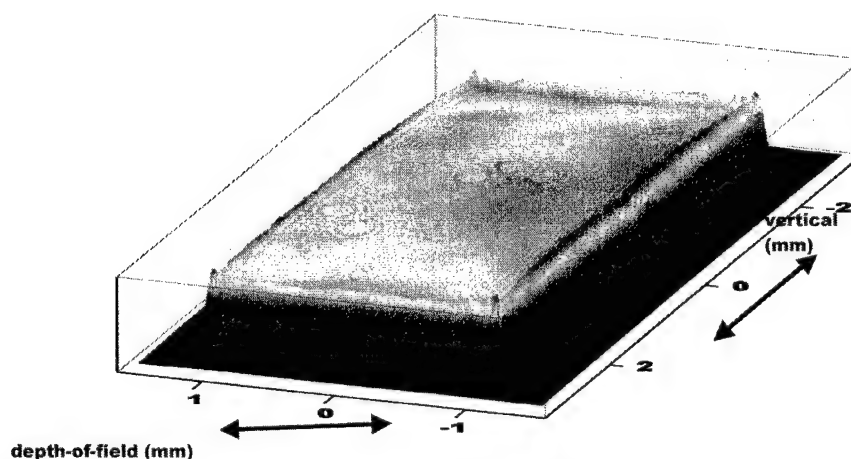
Figure 4: Measured "top hat" beam profile in our LII system.
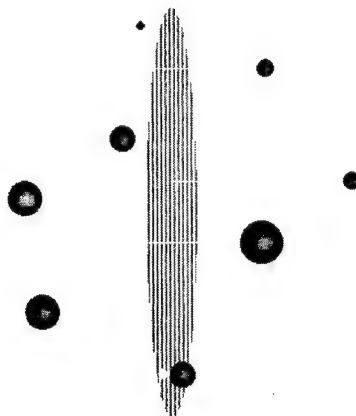
Light Sheetlet

The simultaneous presence of multiple droplets in the probe volume can affect the measurement accuracy. Detailed experimental and theoretical analysis conducted by Sankar and Bachalo has shown that if two droplets are simultaneously present in the PDI probe volume then the Fourier analysis method will result in correct sizing of the larger droplet while ignoring the smaller droplet. As a result, the size distribution can be afffected but the liquid volume flux will be accurately measured. In this Phase I program, we explored other methods to minimize the occurrence of droplet coincidence. The techniques being considered include creation of a light "sheetlet" probe cross-section and advanced signal processing methods:

A schematic of the light "sheetlet" is presented in Fig.5. The key advantages of using a light "sheetlet" probe cross-section are:

- Large target area
- Relatively small probe volume
- Reduces probability of coincidence
- Easily define target area probe cross section definition

Note: Drops within circle would be coincident with a normal circular probe volume
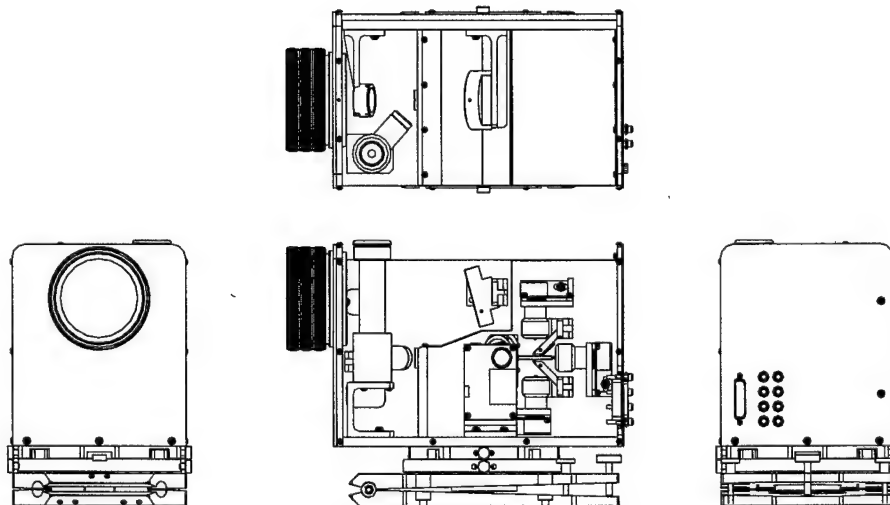

Figure 5: Light "sheetlet" probe cross-section.
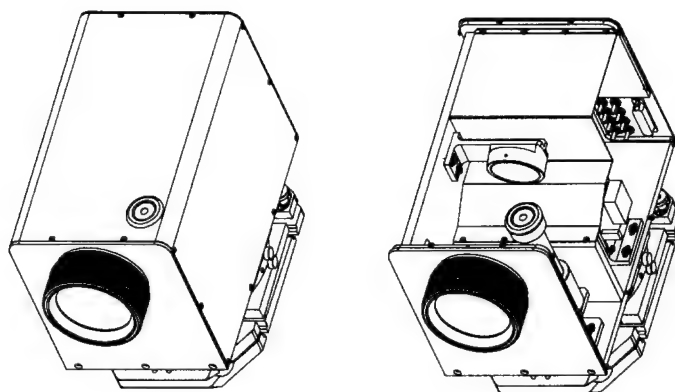
Benchtop PDI Design

A detailed   for a "benchtop" PDI system was developed to experimentally evaluate the effectiveness of the various proposed concepts for improving the accuracy of the PDI measurements. Schematics of the developed design are presented in Figs. 6-8.
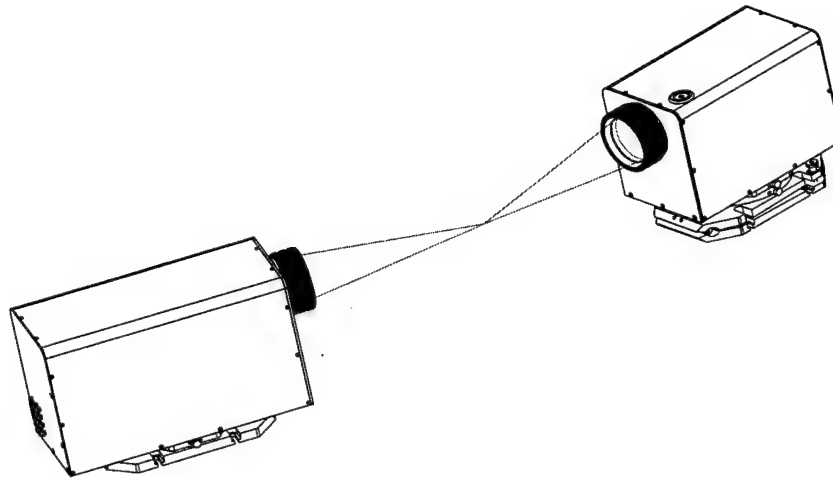
Figure 6: Benchtop PDI design

Figure 7: Details of the benchtop PDI optical receiver.

Figure 8: Details of the benchtop PDI optical receiver.

While the detailed design of the optical receiver for the benchtop PDI system was completed in the Phase I program, the design for the optical transmitter is in progress and will be completed as part of the Phase I Option program. The benchtop PDI system will be thoroughly characterized in the Phase II program and its design will serve as the basis for the cloud probe which will be designed during the Phase II program.

Task 5: Investigate the feasibility of using PC-based signal processing

Conventional PDI systems use dedicated, hardwired signal processors for extracting the frequency and phase information from the Doppler signals and for inferring the particle velocity and size. It is well known from the published literature that the discrete Fourier transform (DFT) provides the optimum method for frequency and phase measurements, especially under low SNR conditions. In the past, the computational burden in computing the Fourier transform has been the main obstacle hindering its application for LDV and PDPA applications where high data rates (in excess of 100,000/sec) with frequencies over a bandwidth of 100 MHz may be encountered. Hardwired FFT processors have been developed but these systems are limited to a fixed record length. Key members of the present research team have extensive experience developing advanced signal processors for LDV and PDI applications. The Doppler Signal Analyzer (DSA) is one Fourier-transform processor developed by this team. This team has also

developed the Real-Time Signal Analyzer (RSA) that incorporates the Gabor and wavelet transforms for providing multiple high-resolution frequency measurements while the Doppler burst is present. The RSA offers tremendous advantage over the DSA in terms of complexity, performance, and cost. However, hardwired processors continue to be the most expensive component of the PDI system.

Over the years, the microprocessor technology has advanced tremendously with respect to processing speed. Microprocessors with speed as high as 2 GHz are readily available for the PC at relatively low prices. Since a PC is a component of the PDI, it would be a tremendous advantage if the role of the hardwired signal processor were changed and the PC could be used for processing the Doppler signals. In such a scenario, the hardwired signal processor assumes the role of detecting the presence of a droplet and then digitizing the Doppler burst and passing it off to the PC for frequency (velocity) and phase (size) extraction.

The feasibility of using this approach was investigated in the Phase I program. Appropriate Fourier transform algorithms and approaches, including frequency-based burst detection methods and phase measurements, were developed and thoroughly investigated. The PC-based signal processor, developed in the Phase I program, has two components to it: (a) the Advanced Signal Analyzer (ASA) hardware, and (b) the Artium Instrument Management System (AIMS) software. Both of these were developed and tested during the Phase I period. A description of the ASA architecture, the signal processing algorithms, the AIMS software, and preliminary data obtained are provided in this section.

Advanced Signal Analyzer (ASA) Architecture:

The architecture of Artium's PDI processor, namely the ASA, was developed to meet the following LDV and PDI measurement requirements:

- Accuracy in frequency (better than 0.1%) and phase (better than 1 degree) measurements. The specified measurement accuracy needs to be achieved even with Doppler signals having very short transit times (approximately 200 ns) and low signal-to-noise ratios (−6dB). Such a

17

stringent measurement requirement necessitates the use of the Fourier analysis method. It is well known in the literature that this method provides optimum results.

- Ability to handle large variations in signal data rate. Data rates can be as low as 1-2 per second to over 100,000 per second. This necessitates the use of a reliable Doppler burst detection circuitry.

- Large variations in transit times - from milliseconds to less than 200 ns. This necessitates the use of adaptive sampling techniques. These techniques require either the sampling frequency or the number of samples per record to be adaptive with the transit time. Optimum results are obtained by using adaptive number of samples.

- Ambiguity in phase measurements is introduced when the sampling frequency is a multiple integer of the Doppler frequency. Innovative sampling digitization techniques are required to resolve this ambiguity in phase measurements.

To meet the foregoing requirements, several innovative techniques for signal digitization and sampling, burst detection, data transfer and signal processing are being incorporated in the ASA.
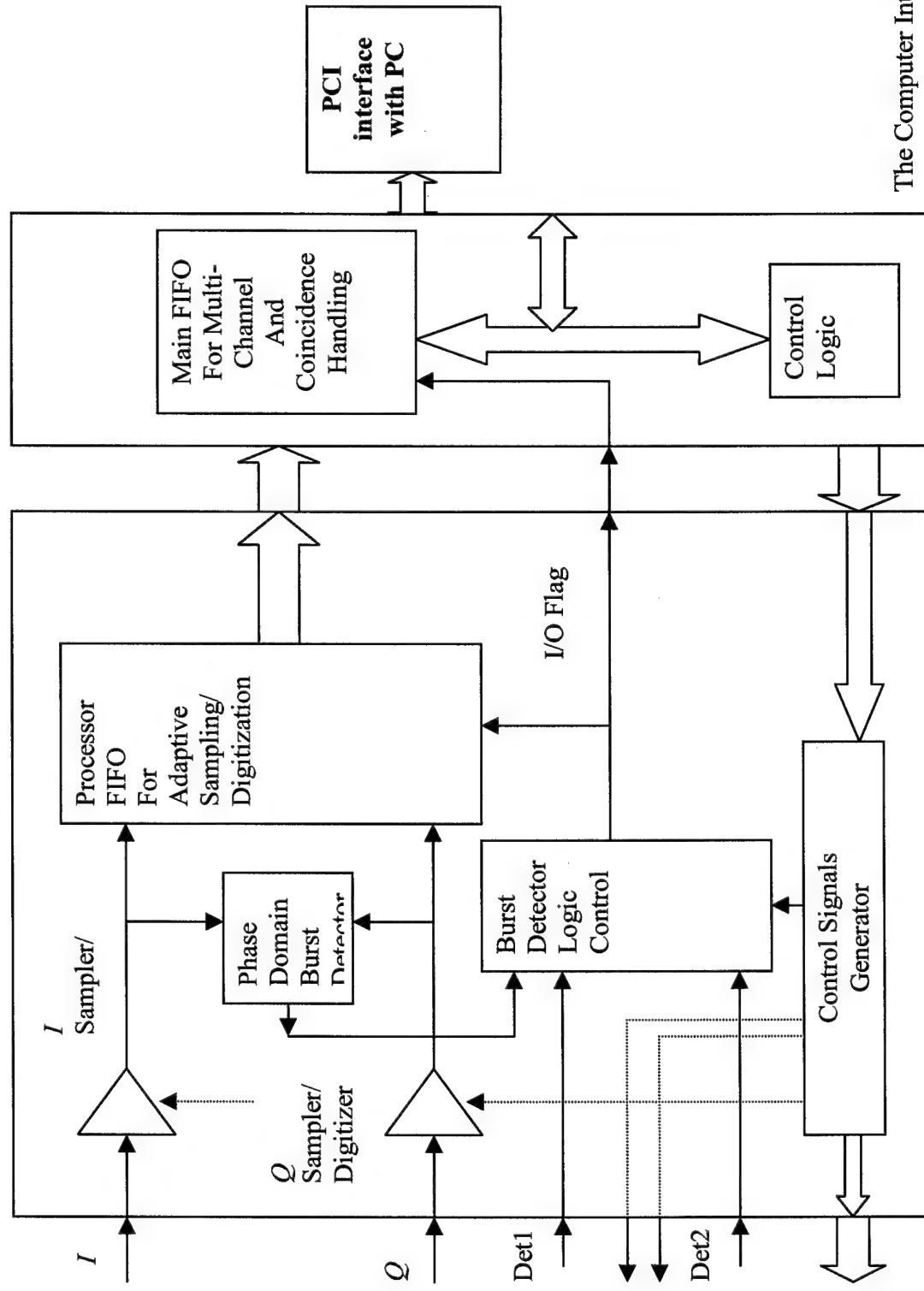
The *Advanced Signal Analyzer (ASA)* comprises of four sections:

1- Photodetection
2- Analog
3- Digital
4- Computer Interface

Figures 9 and 10 show the block diagram for these sections.

Th1 Th2

The Analog Section

The Photodetection
Section
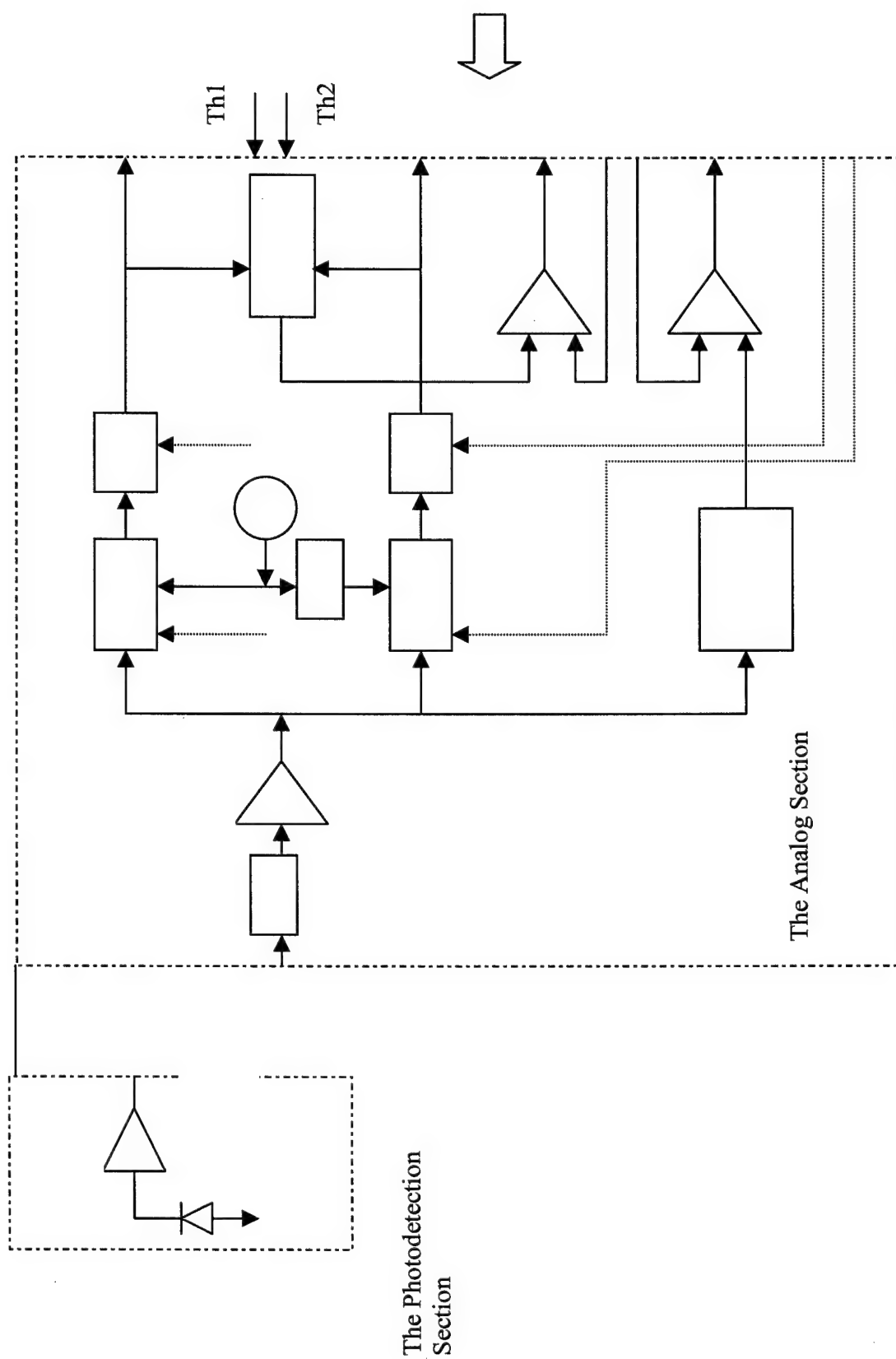
Figure 9 : Block diagram of the photodetection and analog sections.

Figure 10: Block diagram of the digital and computer interface section.

20

The Photodetection Section (PMT/PreAmp Board): In this section, optical signals collected by the PDI optics is converted into current using PMT's or APD's. A transimpedance amplifier is used to convert the photodetector current to voltage. The photodetector section has two outputs. The first one is the raw signal from the transimpedance amplifier. This signal is used for optical calibration and intensity validation. This signal can be used as input for other signal processors in the field like the RSA and DSA. This signal is also high pass filtered and amplified by 15 dB to get the second output of the photodetection section. This output is then fed to the analog section. The photodetection and analog sections can be reconfigured such that the first output (raw signal) is fed to the analog section (as shown in Figure 9). This signal is then high pass filtered and amplified in the analog section.

The analog section (Analog Board): As mentioned in the photodetection section, there are two configurations for the analog section. In the first one (refer to Figure 9), the raw signal output (transimpedance amplifier output) of the photodetection signal is used as an input for the analog section. For this configuration, high pass filtering and amplification by 45 dB are performed in the analog section. The amplified signal is then fed to the quadrature mixer. In the second configuration, high pass filtering and amplification by 15 dB are performed in the photodetection section. This signal is then amplified again by 30 dB in the analog section before it is fed to the quadrature mixer. The second configuration provides better immunity to EMI interference and ground loops and it is the preferred one.

The local frequency of the quadrature mixer (i.e. the mixer frequency) is software selectable. One of six mixer frequencies 40 MHz, 80 MHz, 36 MHz, 30 MHz, variable (10-62.5 in steps of 1Hz) or external can be selected. The use of external mixer frequency allows running all the mixers for multi-channel applications by the signal used for Bragg cell drivers. This provides more accurate near zero velocity measurements.

The two-quadrature mixer outputs (I and Q) are then low pass filtered. There are eight software selectable Low Pass Filters (LPF). These filters are 80, 40, 20, 10, 5, 2.5, 1 and 0.1 MHz. 80 and 40 MHz filters are 5-pole butterfly LPF's. The rest are 3-pole butterfly LPF's. The quadrature outputs of the low pass filter are amplified by 20 dB (or a gain of 10) and then fed to the digital section.

There are two analog burst detectors in the analog section. The first one works on the amplified signal as shown in Figure 9. The amplified signal is applied to the envelope detector (comprises of signal rectification followed by a low pass filter with a time constant of 100ns). The envelope detector output can be used as a measure of the signal average power. It is then compared with a threshold Th1 to get the first analog section burst detector output Det1. The second analog burst detector works on the quadrature LPF outputs (*I* and *Q*). The instantaneous power of the filtered signal $\sqrt{I^2 + Q^2}$ is obtained by squaring the signals *I* and *Q*, summing the squares and determining the square root of the summation. The signal power is then compared with the threshold Th2 to get the second burst detector output Det2. These detector outputs are then fed to the digital section.

The digital section (Processor Board): In this section, the quadrature outputs of the analog section are sampled and digitized. The sampling frequency is software selectable. Eighteen sampling frequencies are obtained by subsequent division of the master clock frequency of 160 MHz by 2. Thus, the sampling frequency ranges from 160 MHz to 1.25 KHz.

The ambiguity in phase measurement when the sampling frequency is a multiple integer of the signal frequency has been resolved by using novel digitizing techniques. With the conventional sampling/digitizing technique, the digitized data repeats itself after a few number of sampling. In this case the processors fails to provide better phase measurements after a few number of samples. With the novel digitizing technique, the digitized data never repeats itself at any signal frequency.

The bit streams from the quadrature digitizer are then applied to the Phase Domain Burst Detector. Unlike the conventional Fourier analysis burst detector (where the hardware complexity increases logarithmically with the number of samples used for burst detection), the new method allows significant increase in the number of samples without increasing hardware complexity. This simplicity in implementation does not compromise performance. Our simulation and initial testing of the newly developed burst detector show that its performance is nearly the same as the optimum performance provided by the Fourier analysis method.

The output of the phase domain burst detector is then combined with the two analog burst detectors to provide the final burst detector output. This output is then fed the adaptive sampling circuitry to store all the signal samples when the burst detector output is active. This means that the number of samples that is dependent on the burst length.

Since the number of samples in the data packet is adaptive with the burst length, the size of the data packet is variable. This requires rigorous synchronizing techniques to avoid the problem of synchronization error. Each data packet will have several synchronization words. Furthermore, each data packet is stamped with two numbers. The first number is the total number of words of that packet and the second is the channel (component) number from which is originated.

Thus the data packet has the following form:
- 2 synchronization words to indicate the start of the data packet. The second word also contains the channel number.
- 1 word to indicate the particle number and the channel number.
- 2 words for the run time.
- 1 word for the transit time.
- 1word to indicate the number of sampled data.
- 2 to 512 of sampled data.
- 1 word for the intensity.
- 0 to 4 words for the external inputs.

Once a data packet is assembled, a valid flag is issued to the computer interface section.

The digital section performs several other functions. These include the measurement of the raw signal intensity, and generating all control signals (analog and digital) for both the analog and digital sections. Analog control signals include analog burst detector thresholds and high voltage controls. Digital control signals include mixer, LPF and sampling frequency selections.

Computer Interface Section (I/O card): The IO card interfaces with the computer via the PCI interface. Once the I/O card detects a valid flag generated by any (maximum of three) of the

processors, it starts serving that particular processor. The valid data packet is then transferred to the main FIFO on the IO card and is then transferred via the PCI interface to the PC memory. The computer unpacks each data packet to recover the sampled data and other information (transit time, elapsed time, intensity) contained in the data packet. The sampled data is then processed using the Fast Fourier Transform algorithm to compute the frequency and the phase. Special algorithms have been devised to improve the frequency and phase resolution in comparison to that provided by the Fast Fourier Transform (FFT). Several validation criteria are used to accept or reject each data packet. This includes the Signal-to-Noise Ratio (SNR) of the sampled data computed using the Fourier Analysis method. In case of size measurement, the SNR for each of the three channels is computed and used to validate the measurement. The intensity is another measurement that is used to validate the size measurement.

Preliminary Specifications for the ASA

Processor bandwidth	5-150 MHz.
Input Voltage	200 uV-1V.
Minimum transit time	100 ns.
Maximum sampling frequency	Quadrature, 160 MHz (equivalent to 320 MHz).
Measurement accuracy: Frequency	0.05 % of the sampling frequency.
Phase	0.5 degree.
Minimum SNR	- 6 dB.
Maximum data rate	250000 per second.
Number of samples	Adaptive 16 to 4096 quadrature (equivalent to 32 to 1024).
Computer Interface	PCI @40 MWords/sec.
Burst Detection	Phase Domain burst detector.
	Quadrature Analog burst detector.
High pass filtering	5,20 MHz.
Low pass filtering	8, Software selectable, 100KHz to 80MHz.
Mixing	6, Software Selectable, 40MHz, 80MHz, 36MHz, 30 MHz, Variable (10MHz to 62.5 MHz at 1Hz step), external.
Bragg cell driver	40 MHz, 0.5 V into 50 Ohm.
Run time	32 bit, 0.5 us resolution.
Transit time	16 bit, 0.1 us resolution.
Coincidence	Hardware, Software.

Advanced Signal Analyzer (ASA) Signal processing Algorithms:

The ASA sampled Doppler burst is processed using the Fourier Analysis method, for which, the accuracies in the frequency and phase measurements are expressed by the Cramer-Rao bound:

$$\text{var}[f] = \frac{12}{(2\pi)^2 \text{SNR} N(N^2 - 1)} f_s$$

$$\text{var}[\phi] = \frac{2(2N-1)}{\text{SNR} N(N-1)}$$

where N is the number of samples, SNR is the Signal-to-Noise ratio, and f_s is the sampling frequency.

For sampled data, the Discrete Fourier Transform (DFT) is computed as follows:

$$X(k) = \sum_{i=0}^{N-1} x(i) e^{-jik/N}$$

where, $X(k)$ is the Fourier Transform of the sampled data $x(i)$ at the frequency $k f_s / N$. The power at this frequency is measured by taking the absolute value of $X(k)$. The frequency of the Doppler signal is then computed by finding k_m or the frequency $k_m f_s / N$, where

$$X(k_m) \geq X(k) \quad \text{for } 0 \leq k < N-1$$

The resolution of the frequency measured by the DFT is given by $1/N$. For N less than 100, the DFT frequency resolution is worse than 1%. However for SNR's greater than –6dB, the Fourier analysis method provides much better resolution as determined by Cramer-Rao bound. To attain higher frequency resolution, the sampled data is padded with *(K-N)* zeros. The DFT of the sampled data with padding is then given by:

$$X(k) = \sum_{i=0}^{N-1} x(i) e^{-jik/K}$$

where, K is the total number of DFT points. Using the above equation, the resolution of the new DFT is then given either by the Cramer-Rao bound for noisy signals or $k_m f_s / K$ for good SNR signals.

It should be pointed out that the number of sampled data N is a variable that can be read from the data packet. This number depends on the transit time and the sampling frequency. The number K is a software parameter that can be selected by the user with a default value of 1024. For K=1024, the frequency resolution is equal to or less than 0.1% of the sampling frequency. The user may increase this number to obtain higher frequency resolution at the expense of processing speed. Since N is a variable, the number of padded zeros $(K-N)$ varies from sample to sample. For $N > K,$ K samples around the center of the burst are chosen to ensure optimum results.

The FFT method is used to compute the DFT for each sample record. The frequency of the Doppler signal is then computing by finding the number k_m or the frequency $k_m f_s /K$ where,

$$X(k_m) \geq X(k) \quad \text{for } 0 \leq k < K - 1$$

This measurement is then validated by computed the SNR. Thic can be achieved by computing the Doppler signal power at the frequency $k_m f_s /K$ and dividing it by noise. The noise is computed by subtracting this number from the total signal power. Alternatively, one may compute the Doppler signal power to the total signal power and use the result for validation. This Doppler Signal Power (DSP) to the Total Signal Power (TSP) is given by:

$$DSP/TSP = \frac{X(k_m)}{\sum_{i=0}^{N-1} |x(i)|^2}$$

This number is then compared with a threshold to reject signals with SNR's lower that a certain threshold. For minimum SNR's of –6 dB, the Doppler signal power to total signal power should be greater than 0.2.

The number k_m plays an important role in phase measurement. This number is used to generate a reference complex sinusoidal wave with a frequency of $k_m f_s /K$. This complex wave is then

correlated with each of the three channels complex signals. The phase of each of the incoming signals with respect to the reference signal is then given by:

$$\theta_c = \tan^{-1}\left\{\frac{\sum_{i=0}^{N-1}\left[I_c(i)\cos(2\pi i k_m/K)+Q_c(i)\sin(2\pi i k_m/K)\right]}{\left[\sum_{i=0}^{N-1}\left[-I_c(i)\sin(2\pi i k_m/K)+Q_c(i)\cos(2\pi i k_m/K)\right]-\right]}\right\}$$

where c= 1, 2 or 3 and refers to the channel number. The phase difference between channels 1 and 2 is then given by:

$$\theta_{12} = \theta_2 - \theta_1$$

and the phase difference between channels 1 and 3 is given by:

$$\theta_{13} = \theta_3 - \theta_1$$

Each phase measurement is then validated by computing the Doppler signal power to the total signal power for each of the three channels. This ratio should be greater 0.2 for –6dB minimum SNR for all the three channels. For the phase measurement to be validated, this ratio should be higher than the threshold for all the channels.

Artium Instrument Management Software (AIMS)

This section provides an overview of the Artium Instrument Management Software (AIMS) that is used to acquire and process the PDI data. The Artium Instrument Management Software (AIMS) package is a client-server system that fully controls all aspects of PDI (Phase Doppler Interferometry) acquisition and processing. Unlike competing software packages, AIMS features software-based signal analysis and user-extendable options.

Client-Server Architecture

Unlike most data acquisition software, the Artium Instrument Management Software (AIMS) uses the client-server model. The user interacts with the client program, which connects through a network connection to the data server. The data server controls acquisition devices (like the Advanced Signal Analyzer, or ASA, for PDI), manages data storage, and performs all calculations. The ADMS client-server concept offers several advantages:

- *Access data from anywhere.* Since the client and server need only be connected via a network (like an Intranet or the Internet), data can be viewed anywhere the client software is installed. The client software supports the Windows (95/98/Me/NT/2000/XP), Solaris, and Linux platforms.

- *Easy data sharing.* Multiple clients can connect to the server at once, so data is now a shared resource. The data server limits access to the acquisition devices so that only one user can acquire data at a time, but different clients can access the same data simultaneously.

- *Remote instrument operation.* Since the client and server programs do not need to be located on the same computer, data acquisition and instrument control can be performed remotely. Artium has tested this capability extensively, and have acquired data from a partner's instrument in Ottawa, Canada from our offices in California.

Client Software Overview

The client software is comparable to a web browser. Like a web browser, the client connects to a server for data. Like a web browser, the client is responsible for displaying data and results to the user.

PDI Processing

Traditionally, PDI processing was performed in fixed (hard-wired) hardware processors. This hardware-only approach was necessary since typical personal computers (PCs)/workstations did not have enough processing power to complete analyses/calculations in a reasonable amount of time. As the table shows, PCs have exponentially increased in clock speed over the past twenty

28

years (clock speed is a rough indicator of processor power). Artium has tested the software with currently-available 1-2 GHz computers and found the computational power to be more than sufficient.

Year	Processor	Maximum Clock Speed (MHz)
1971	Intel 4004	0.108
1972	Intel 8008	0.2
1974	Intel 8080	2
1978	Intel 8086	10
1982	Intel 286	12.5
1985	Intel 386	33
1989	Intel 486	50
1993	Intel Pentium	66
1997	Intel Pentium II	300
1999	Intel Pentium III	1200
2000	Intel Pentium 4	2400

In the Artium PDI system, the ASA processor is responsible for detecting and digitizing the incoming Doppler signals. All of the settings for the ASA are controlled via the Artium software. The processor passes the digitized Doppler signals to the software through a custom PCI (Peripheral Connect Interface) interface card. The card contains an on-board FIFO (First In, First Out) buffer, and is capable of transferring data to the computer memory at speeds up to a maximum of around 130 Mbits/second. The interface card buffer and high data transfer rates ensure there is no loss of incoming data. The interface card uses DMA (Direct Memory Addressing) to transfer the raw data to the computer's memory, which reduces the load on the main CPU (Central Processing Unit, the "brains" of the computer).

Once the raw data is in the computer memory, a device driver (a piece of low-level code that is the interface between the card and the Artium Data Server) buffers the data once again. When new data arrives, the device driver notifies the Artium Data Server. When the Data Server software is ready, it reads the raw data from the device driver.

Depending on the data the Client software wants to display, the Data Server performs the needed calculations on the raw data and passes the processed results to the Client software. For PDI, this processing includes:

- Parsing the raw data into signal-sized packets
- Determining the frequency of the Doppler signals
- Determining the phase shift between the Doppler signals
- Validating frequency and phase shift values

As mentioned previously, other signal processors typically perform these steps in specialized electronic hardware.

Advantages to PC-based Signal Processing

Raw data can be reprocessed. With a hardware approach to signal processing, the algorithm for analyzing data is fixed, which means that compromises must be made (speed for accuracy, etc.). With software-based signal processing, the raw data can be reprocessed multiple times, using different algorithms or parameters, offering more flexibility. Other companies have tried programming DSPs (Digital Signal Processors) to provide for flexibility in processing, but once the data has been processed by the DSP, the raw data is lost, so different algorithms/approaches cannot be tried on the same set of data.

PC Computational abilities are still increasing. A fixed, hardware-based processor is limited to the same processing speed as when it was manufactured. With software-based processing, the

processing speed can be increased by upgrading to a faster CPU or by adding more networked computers (parallel processing – this feature is not yet implemented or planned).

Improved testing. Software-based processing can be tested with simulated signals. These signals are generated by a variety of means, but can be stored and reproduced easily. This allows automated testing of the processing calculations, and means the ASA processor and interface card are not necessary for testing.

With a hardware-based processor, testing must include a hardware signal simulator connected to the processor. Unlike simulated signals, hardware-generator signals have some variability and are very difficult to test in an automated fashion.

Simpler hardware. In a software-based approach, much of the calculation complexity is shifted to the software, meaning the ASA processor can be simplified. Simplification leads to fewer hardware bugs (which are more difficult to fix than software bugs) and a lower manufacturing cost for the processor.

More validation and calculation steps are available. A hardware processor sends the processed data to the computer/software, so there are a number of processing steps that are unavailable (since the complete signal has been lost). Some lost possibilities with a hardware-based approach are:

- Better determination of coincident signals (this occurs when two or more particles are in the probe volume at the same time).
- Processing of coincident signals. Currently, information about coincident particles is rejected, but we feel it may be possible to process and retrieve information about the particles.
- Elimination of trajectory-dependent errors. We are investigating a method to dramatically reduce or eliminate trajectory-dependent sizing errors.

Extensibility

The client and software programs have been designed to be extended and modified by the end-user.

Basic Modifications

Basic modifications to the programs do not require any programming expertise, but currently need an understanding of the software.

Data display layouts. The data display screens are setup with a text file. While we envision an online screen editor, users can currently create and edit screen files. This allows users to customize data displays for their particular application, adding needed information and removing superfluous items.

Calculation templates. The order and input to all calculations on the data server are controlled with calculation template files. These files specify the calculations to be used and the inputs to the calculations. By editing these files, users can change the order or add new calculations to the processing path. Eventually we plan to develop a graphical interface for users to modify calculation templates.

Advanced Modifications

Advanced modifications require programming (in the Java language). Tools for these modifications are freely available. Artium can provide programming support for advanced modifications.

New screen objects. There is a well-defined API (Application Program Interface) for creating new objects to display data on the screen. Existing examples of screen objects are tables, fields, and graphs.

New calculations. As with screen objects, there is a well-defined API for creating new calculations. Users can create new calculations and have these interact with or replace existing calculations. Instead of exporting data and then analyzing it in another program, users can implement the calculation in the data server, so it is available in the client data display with the default set of calculations.

Testing and Validation.

This section describes some of the testing and validation steps that Artium has performed on the PDI software/hardware.

Software Unit Testing

Unit testing is a process where a program unit is fed data and the output is compared to known results. For example, a frequency calculation would be input a signal of a known frequency, and the resulting frequency would be compared with the known input frequency.

The data server calculations incorporate unit testing as a first check of validity. These unit tests also offer confidence that modifications to the calculations do not affect the correctness of the calculations.

Data Rate and Throughput

Artium has a hardware Doppler signal generator. This generator is able to produce Doppler signals up to a maximum data rate of about 117kHz, which is greatly in excess of any real-world data rate. Using this simulator, we were able to verify the PDI processing system of ASA, interface card, computer and data server software can handle high data rates without losing data.

Actual Data

The disadvantage to the current Artium hardware signal generator is that the system can produce signals at a constant Doppler frequency. The frequency can be changed manually, but not in a predictable way.

To test the system with real data, Artium used an existing Aerometrics PDPA (Phase Doppler Particle Analyzer) optical system with a simple pressure atomizer. The system currently uses an Aerometrics RSA (Real-time Signal Analyzer) and DataVIEW software, so it was possible to directly compare results with the Artium processing system.

Preliminary testing at Stanford University

The prototype ASA was tested at the Stanford University in a simple spray application. Typical size and velocity histograms are presented in Figs. 11 and 12, respectively.
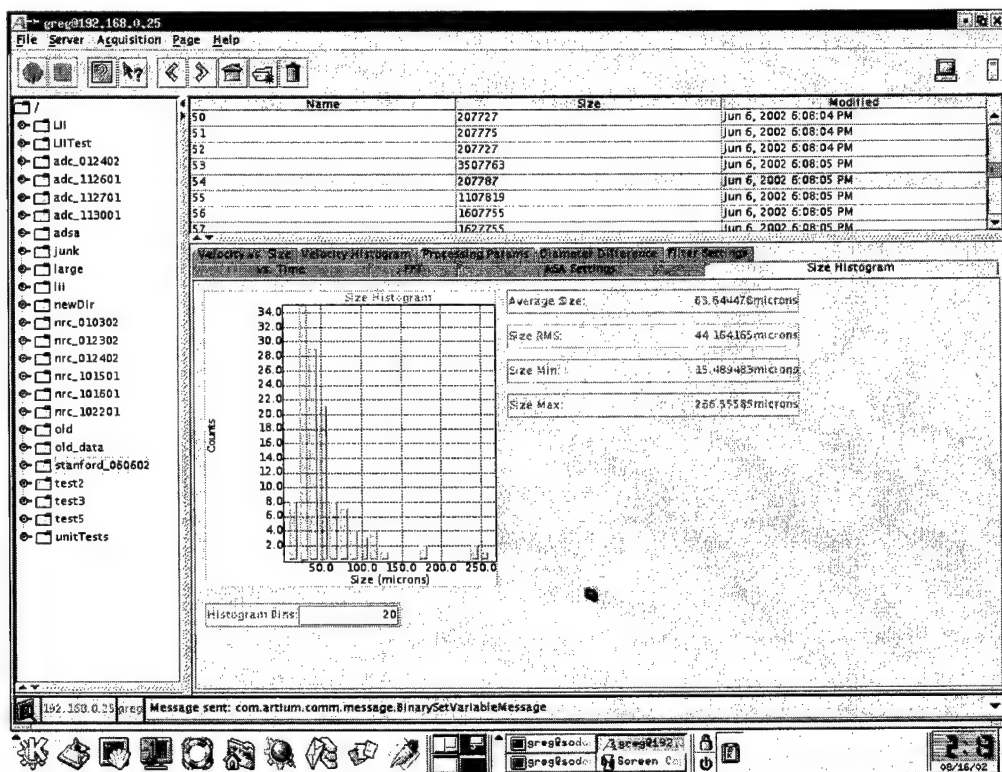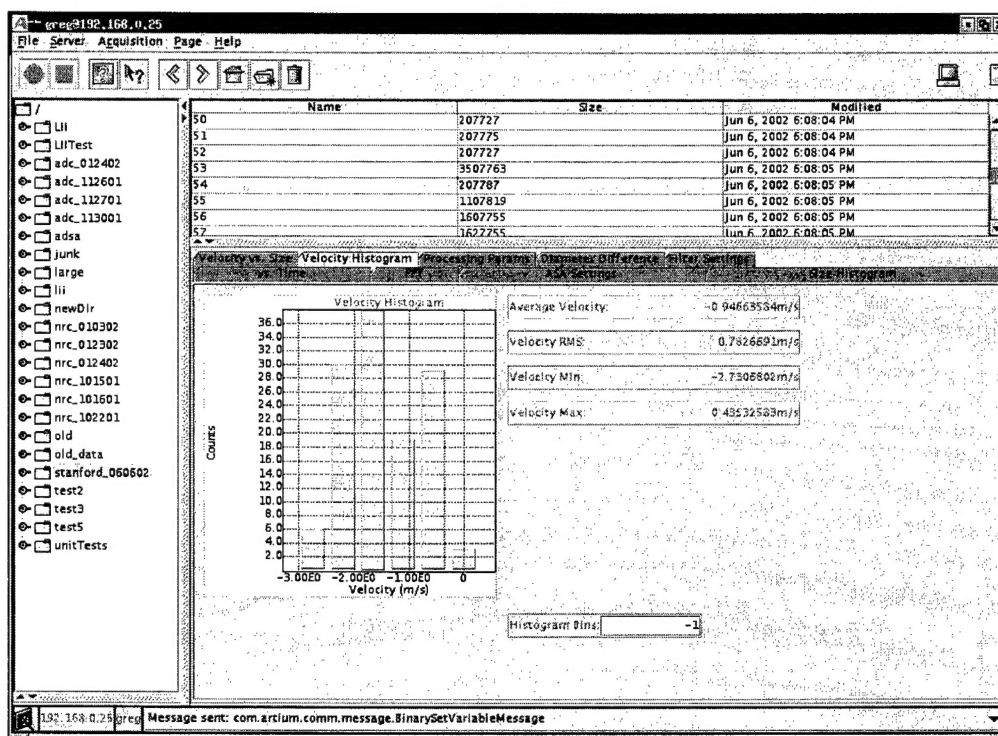

Figure 11: Measured droplet size histogram.

Figure 12: Measured droplet velocity histogram.

The results obtained with the ASA was compared with that of the RSA and the two of them were in excellent agreement clearly validating the ASA design.

Autosetup

One of the criticisms of the Phase Doppler instrument has been the effect of system settings on the acquired results:

Problem	Result
Gain (high voltage) set too low	Smaller particles are not measured
Processor sampling rate set too low	Higher frequency (faster particles) are measured wrong
Processor sampling rate set too high	Lower frequency (velocity) resolution

Experienced users of PDI tend to use loose set of rules to determine a good values for a given experimental setup. However, this process is iterative and somewhat tedious, so many users

35

select one setup and use it even when the conditions of the experiment change (making the instrument setup invalid). Additionally, most users are not interested in becoming experts in the theory and operation of PDI – they want to use the system to obtain (correct) results for their application.

Auto-setup is a process where the software (AIMS) decides on the best system settings for a given application. Before acquiring data, AIMS samples the incoming data and analyzes the results. Based on this preliminary analysis, AIMS uses a set of algorithms to pick the best settings for the current application. Auto-setup removes the burden of instrument setup from the user and ensures the measured results are correct. Additionally, when the experimental conditions change, auto-setup changes the instrument settings appropriately.

The basic algorithm for the autosetup was developed and tested during the Phase I program. This feature will be further expanded and tested for robustness during the Phase II program and will be an essential element for the PDI cloud probe.

Task 6: Methods to reduce droplet coincidence

PDI is a single particle measurement technique, and droplet coincidence, the presence of more than one droplet in the optical view volume at a given time, plagues many existing instruments. In the Phase I program, we explored methods for minimizing the probability that more than one droplet exists in the probe volume at a given moment. Specifically, we investigated the use of laser light sheets as a means to minimize the measurement probe volume and hence the coincidence. The details of this technique was provided earlier. We have currently employed this approach in another instrument of ours, namely the LII system for soot characterization, and have already incorporated it into the design for the benchtop PDI system. Detailed characterization will be undertaken in the Phase II program.

Task 7: Investigate suitable means for discriminating between solid ice-crystals and liquid drops.

The PDI system requires the droplets to be spherical, predominantly reflective or refractive in nature, and its refractive index to be known. In supercooled clouds, it is possible that both ice

crystals and liquid drops are simultaneously present. This could pose a problem because the light scattering characteristics of the ice crystals will be different from the liquid drops and hence this could lead to measurement error. This is highly unlikely to be a problem in warm clouds, but is an important issue for mixed-phase clouds. In addition, we have already discussed the scientific benefits of having a means for discriminating between the particle phases. Therefore, we had proposed to investigate the feasibility of incorporating means for detecting whether individual particles are liquid drops or ice crystals.

One possible method for differentiating between the two phases is to examine the polarization characteristics of the scattered light. The solid ice crystals, because of their surface irregularity and also because of high reflective component, are expected to depolarize the incident polarized laser light. On the other hand, the liquid drops are expected to have a smooth surface. As a result, the scattered light will maintain the polarization of the incident laser beams. Two detectors with different polarizers in front of them will be used to monitor the extent of scattering in two orthogonal polarization directions. This information will then be used to decide if the particle is a liquid droplet or an ice crystal. The PI and his team has already patented and built a sensor using this principle for differentiating between snow and rain.

We started investigation of this approach and will further explore it during the Phase I Option period.

Task 8: Development of a novel particle imaging probe

During the Phase I we investigated various high speed, 2-D CCD cameras for use in a particle imaging probe. We have identified a camera from Dalsa Corp. which offers 256 x 256 pixels at nearly 1 kHz frame rate. We are working with Dalsa to get an evaluation unit. This unit will be evaluated along with the benchtop PDI system during the Phase I Option and the Phase II periods.

REPORT DOCUMENTATION PAGE

Public reporting burden for this collection of information is estimated to average 1 hour per response, including the time for reviewing instructions, searching existing data sources, gathering and maintaining the data needed, and completing and reviewing the collection of information. Send comments regarding this burden estimate or any other aspect of this collection of information, including suggestions for reducing this burden, to Washington Headquarters Services, Directorate for Information Operations and Reports, 1215 Jefferson Davis Highway, Suite 1204, Arlington, VA 22202-4302, and the Office of Management and Budget, paperwork Reduction Project (0704-0188), Washington, DC 20603.

1. AGENCY USE ONLY (Leave Blank)	2. REPORT DATE	3. REPORT TYPE AND DATES COVERED
	November 12, 2002	Final Report; June 1, 2002 – September 30, 2002

4. TITLE AND SUBTITLE	5. FUNDING NUMBERS
Development of an airborne integrated phase Doppler interferometer/imaging probe for accurate cloud droplet size distribution measurement	N00014-02-M-0153

6. AUTHOR(S)

William D. Bachalo and Subramanian V. Sankar

7. PERFORMING ORGANIZATION NAME(S) AND ADDRESS(ES)	8. PERFORMING ORGANIZATION REPORT NUMBER
Artium Technologies, Inc. 150 West Iowa Avenue, Suite 202 Sunnyvale, CA 94086	

9. SPONSORING/MONITORING AGENCY NAME(S) AND ADDRESS(ES)	10. SPONSORING/MONITORING AGENCY REPORT NUMBER
Office of Naval Research 800 North Quincy Street Arlington, VA 22217-5660	

11. SUPPLEMENTARY NOTES

12a. DISTRIBUTION/AVAILABILITY STATEMENT (see Section 5.3b of this solicitation)	12b. DISTRIBUTION CODE
Unlimited/Unclassified	

13. ABSTRACT (Maximum 200 words)

The Phase I effort investigated the feasibility of developing an optical probe based on phase Doppler interferometry (PDI) for reliable and accurate measurement of the cloud droplet size distribution from airborne platforms. The key features of this device are high accuracy and precision droplet sizing, large dynamic range, accurate concentration measurement throughout the entire instrument dynamic range, very low coincidence errors, and large counting volume.

14. SUBJECT TERMS		15. NUMBER OF PAGES
Cloud probe; phase Doppler interferometry; droplet sizing		36
		16. PRICE CODE

17. SECURITY CLASSIFICTION OF REPORT	18. SECURITY CLASSIFICATION OF THIS PAGE	19. SECURITY CLASSIFICATION OF ABSTRACT	20. LIMITATION OF ABSTRACT
Unclassified	Unclassified	Unclassified	Unlimited